

Nanoneedles of Lanthanum Oxide (La_2O_3): A Novel Functional Material for Microwave Absorber Material

This content has been downloaded from IOPscience. Please scroll down to see the full text.

2017 IOP Conf. Ser.: Mater. Sci. Eng. 202 012066

(<http://iopscience.iop.org/1757-899X/202/1/012066>)

View [the table of contents for this issue](#), or go to the [journal homepage](#) for more

Download details:

IP Address: 223.25.97.66

This content was downloaded on 02/06/2017 at 02:36

Please note that [terms and conditions apply](#).

You may also be interested in:

[Microwave Dielectric Properties of Lossy Dielectric Composite Materials](#)

Young Joon An, Hirotake Okino, Takashi Yamamoto et al.

[LANTHANUM IN VARIABLE STARS IN CLASS N](#)

Roscoe F. Sanford

[Short range structure of lanthanum chloride/oxychloride determined by EXAFS](#)

H Matsuura, S Watanabe, T Kanuma et al.

[Synthesis and Characterization of Microwave Absorber \$\text{SiO}_2\$ by Sol-Gel Methode](#)

S Wardiyati, W A Adi and Deswita

[Investigation of the argon arc binding to the lanthanated tungsten cathode](#)

M. Kh. Gadzhiev, M. A. Sargsyan, D. V. Tereshonok et al.

[Interface Reaction of a Silicon Substrate and Lanthanum Oxide Films Deposited by Metalorganic Chemical Vapor Deposition](#)

Hirotohi Yamada, Takashi Shimizu and Eiichi Suzuki

[Effect of \$\text{La}_2\text{O}_3\$ addition on structural and electrical properties of sodium borosilicate glasses](#)

V Y Ganvir and R S Gedam

[The study of the thermal stability of \$\text{Ni}_3\text{Al}\$ nanoneedles using computer simulation](#)

G M Poletaev, M D Starostenkov, D V Novoselova et al.

[Twin step synthesis of lanthanum zirconate through transferred arc plasma processing](#)

S Yugeswaran, V Selvarajan, P V Ananthapadmanabhan et al.

Nanoneedles of Lanthanum Oxide (La_2O_3): A Novel Functional Material for Microwave Absorber Material

W A Adi, S Wardiyati and S H Dewi

¹Centre for Science and Technology of Advanced Materials, BATAN, Kawasan Puspipstek Serpong Tangerang Selatan Banten, Indonesia

Email: dwisnuaa@gmail.com

Abstract. Synthesis and characterization of La_2O_3 nanoneedles have been successfully carried out by using hydrolysis reaction with NH_4OH as a solvent. La_2O_3 was prepared from LaCl_3 solution. LaCl_3 was preheated on a hotplate and stirred by using a magnetic stirrer, then added solution of NH_4OH 1 M with the variation speed drops of 3 ml, 6 ml and 9 ml to obtain white precipitation $\text{La}(\text{OH})_3$ until a pH of 9. Stirring was continued until 1 hour. A white precipitate formed is separated from the effluent by centrifugation method with 3000 rpm and neutral pH. Then, the precipitate was dried in an oven at a temperature of 70 °C and sintered at 1000 °C to get La_2O_3 nanoneedles. The identification of sample phase was carried out by using X-ray diffractometer (XRD). The refinement results of X-ray diffraction pattern shows that the samples have a single phase of La_2O_3 . The morphology of the nanoneedles was observed by using the transmission electron microscope (TEM). Meanwhile, the reflection and transmission of electromagnetic wave were measured by using the vector network analyzer (VNA) at X-band frequency.

Keywords: Lanthanum oxide, nanoneedle, rare earth, microwave absorber.

1. Introduction

Rare earth metals consist of 15 elements in the lanthanide group from the periodic table, however, scandium (Sc) and yttrium (Y) can be categorized as rare earth metals the similarities in nature and also the existence in nature tend to be along with elements of the lanthanide. Rare earth metals in Indonesia are found in the mineral monazite which is associated minerals incorporated with lead and radioactive element [1-2]. Because as a by-product of tin processing results then only sold at very cheap prices, even at some points thrown away, whereas in the mineral contained rare earth elements having high sales value and much needed in some industries. The dominant elements of rare earth mineral contained in monazite are lanthanum (La), cerium (Ce), neodymium (Nd) and praseodymium (Pr) [3]. The economic potential of monazite previously into tin mining by-products can be increased as added value which is in line with their needs as large as the raw material of advanced industry, in addition to the China policy about export restrictions for the rare earth metals.

Recently, utilization of the rare earth metals is very spacious, especially in the development of high technology. Europium (Eu) is used for computer monitors, erbium (Er) for a cable of fibre optic, neodymium (Nd), samarium (Sm), gadolinium (Gd), dysprosium (Dy), and praseodymium (Pr) for permanent magnets, while lanthanum (La) has been applied widely as functional magnetic materials. There is much more utilization of LTJ which has not been replaced by another material yet [4-6].



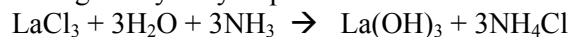
An interesting case to be studied is the use of nanoparticles of lanthanum oxide as absorbing microwaves [7-10]. Lanthanum (La) is the lightest element in the lanthanide group, and has been widely studied in the form of oxides, hydroxides, and phosphates. Various chemical methods have been used to make nanostructures of lanthanum oxide. Synthesizing La(OH)₃ nanotubes has been succeeded through hydrothermal method. La(OH)₃ nanorods have been made through chemical methods. In addition, and a simple method to make La(OH)₃ nanowires has been reported [11-16].

This research will perform the synthesis of lanthanum oxide which focuses on the process of forming nanoneedles. The method used is a hydrolysis method. In addition, this section also discusses the factors that influence during the synthesis process namely pH value and temperature. So, it is expected to find the factors that play role important in controlling the morphology of these nanoneedles. Besides, this paper will present several challenges of scientific with respect to further investigation about microwave absorption capability at this material.

2. Experimental Method

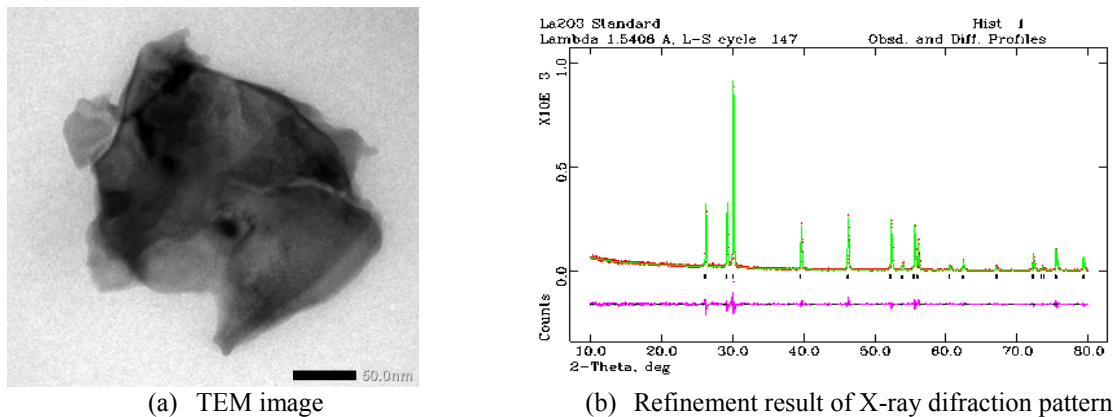
Powders of La₂O₃ were synthesized by the hydrolysis method. The raw materials used were a solution of LaCl₃ and ammonia. The first stage of the process conducted for this synthesis was the solution of LaCl₃ was heated by using a hotplate at a temperature of 80 °C and stirred by using a magnetic stirrer with a speed of 70 rpm, then added with a solution of ammonia of 1 M by using a peristaltic pump with variations of drops speed of 3 ml/min, 6 ml/min and 9 ml/min for the deposition process up to reach a pH of 9. Stirring was continued for 1 hour. The third of white precipitate formed is separated from the effluent through the method of centrifugation at 3000 rpm until the pH back to neutral. Then the precipitate was dried in an oven at a temperature of 70 °C. After that, the precipitate furthermore was sintered in the electric chamber furnace at 1000 °C for 5 hours to obtain crystalline powder of La₂O₃ materials.

The reactions that occur during the hydrolysis process are as follows:



The particle morphology of La₂O₃ powder resulting from differences in drops speed of 3 ml/min, 6 ml/min and 9 ml/min was observed by using a transmission electron microscope (TEM) JEOL brand. Meanwhile, the phase identification of the three samples was characterized by using X-ray diffraction (XRD) Analytical Pan brand with CuK α radiation ($\lambda = 1.5406 \text{ \AA}$). The crystal structure analysis of the sample is calculated based on analysis by using the Rietveld method namely GSAS programs (general structure analysis system) to determine the crystal structure parameters of each sample and the presence of crystal growth in the hydrolysis process results [17]. The calculating electromagnetic wave absorption in this material was by using a vector network analyzer (VNA) with a frequency range of 8-12 GHz (X-band).

3. Results and Discussion



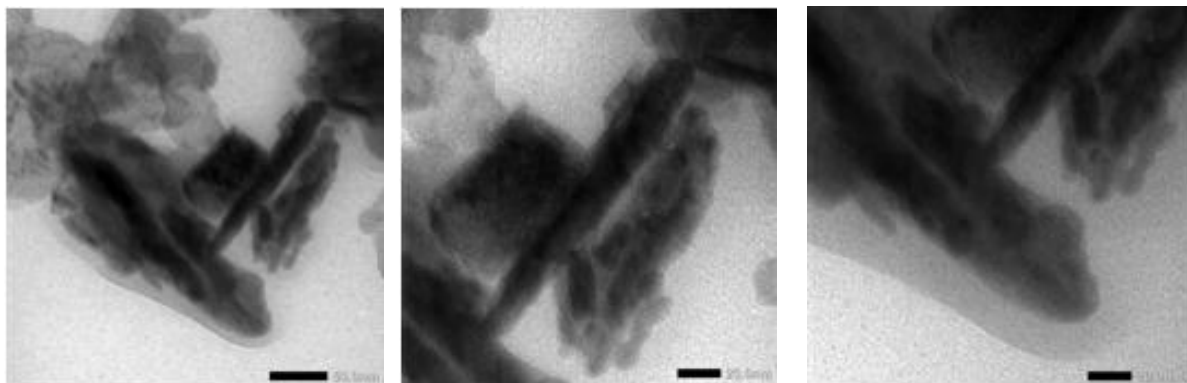
(a) TEM image

(b) Refinement result of X-ray diffraction pattern

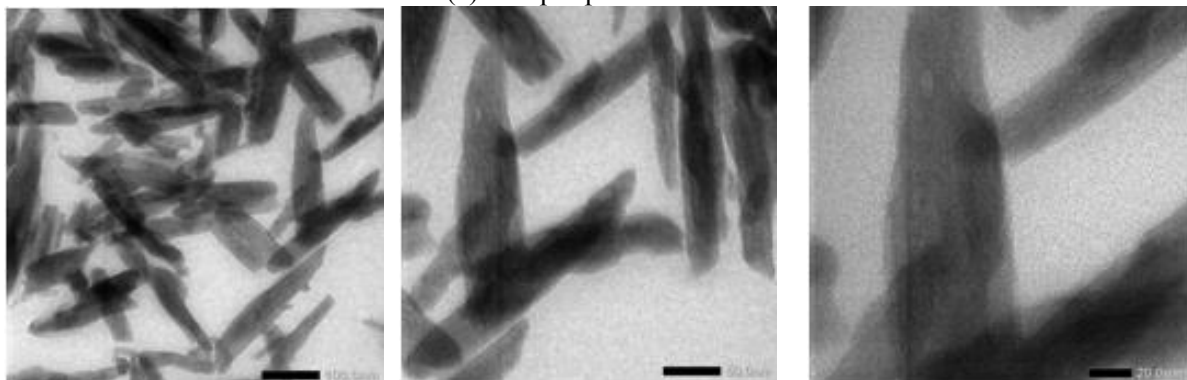
Figure 1. Morphology and phases analysis of La_2O_3 nanoparticle

At the beginning of this study, the the nanoparticles morphology of La_2O_3 commercial product (standard) was observed to get a general idea about particle morphology of La_2O_3 . This morphological observation using a transmission electron microscope (TEM) with a magnification scale of 50 nm is shown in Figure 1(a).

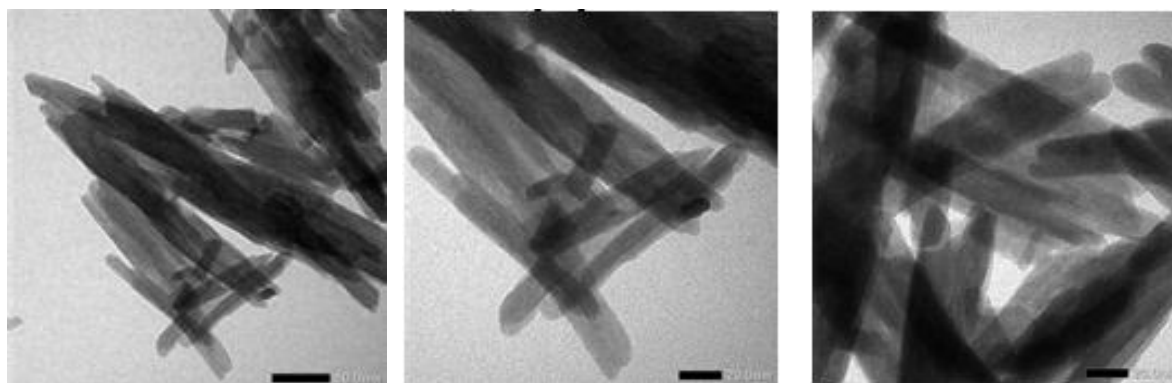
Figure 1(a) shows nanoparticles morphology of La_2O_3 standard in which polygonal solid shaped with particle sizes was around 200 nm. The interesting thing about the image that the polygonal shape is a basic form of nanoparticles La_2O_3 corresponding to the shape of this crystal structure. The measurement results of X-ray diffraction pattern of the standard La_2O_3 nanoparticles is shown in Figure 1(b).



(a) Drops speed of 3 ml/min



(b) Drops speed of 6 ml/min



(c) Drops speed of 9 ml/min

Figure 2. Nanoparticles morphology of La_2O_3 nanoneedles

The refinement of XRD profile for La_2O_3 standard as shown in Figure 1(b) appears that the fitting X-ray diffraction pattern has a very good fitting quality based on the criteria of fit (Rwp) and goodness of fit (χ^2) in accordance with the agreement [17]. Rwp is the weight ratio of the difference between the XRD pattern of observation and calculation (ideal value of Rwp < 10%). Meanwhile, χ^2 (chi-squared) is the ratio of the XRD pattern of observation results comparable with expectations (ideal value of $1 < \chi^2 < 1.3$). The refinement results of x-ray diffraction pattern confirmed that the sample is a single phase of La_2O_3 with a hexagonal structure, space group of P 63/m m c, meanwhile, the unit cell parameters for the La_2O_3 phase is summarized as the following: $a = b = 3.9346(1) \text{ \AA}$ and $c = 6.1265(1) \text{ \AA}$, $\alpha = \beta = 90^\circ$ and $\gamma = 120^\circ$, $V = 82.13(1) \text{ \AA}^3$, $\rho = 5.030 \text{ gr.cm}^{-3}$, wRp = 6.7% and χ^2 (chi-squared) = 1.14. The results of nanoparticle morphology is similar to the results of research of Mazloumi [18] who has managed to make nanostructure lanthanum hydroxide powders by using chemical process with KOH and NaOH as the solvents.

However, the process result of this hydrolysis has different morphological forms. The TEM image observations have obtained the morphology of La_2O_3 nanoparticles shaped nanoneedles. Figure 2 shows the morphology of La_2O_3 nanoneedles according to a drops speed of 3 ml/min, 6 ml/min and 9 ml/min ammonia. The looks growth occurs on the specific field orientation in the La_2O_3 crystal. Figure 2(a) is a TEM image of La_2O_3 nanoneedles with the drops speed of 3 ml/min. It appears that the growth of La_2O_3 nanoneedles has been successfully formed although there are still several different particle shapes. This phenomenon needs to be confirmed based on the analysis phases result of the X-ray diffraction pattern. La_2O_3 nanoneedles formed has a diameter of 30 nm by variation of the length in ranges from 50-150 nm. Figure 2(b) is a TEM image of La_2O_3 nanoneedles with the drops speed of 6 ml/min of which growth results shape was much better compared with the results of the drops speed of 3 ml/min.

At drops speed of 3 ml/min, La_2O_3 nanoneedles formed has a shape and size that are relatively uniform in which particle diameter is 20 nm and an average length around 250 nm. However, these particles seem still wrapped with the form of other particles so they need also confirmation with the results of phase analysis by using XRD. Figure 2(c) is a TEM image of La_2O_3 nanoneedles synthesized with the drops speed of 9 ml/min. At this speed, the results of nanoneedles obtained relatively looks better compared to the drops speed of 3 and 6 ml/min. Nanoneedles morphological forms appear more clearly and relatively homogeneous. Average diameter of particle is about 10 nm with an average length of about 250 nm. The interesting case in this study is the changing shape of the particles from polygonal shape into nanoneedles. This case means that the preferred orientation (PO) of crystal is thought to occur in the direction of a particular field so that an understanding of the crystal structure and phases analysis needs to be studied further.

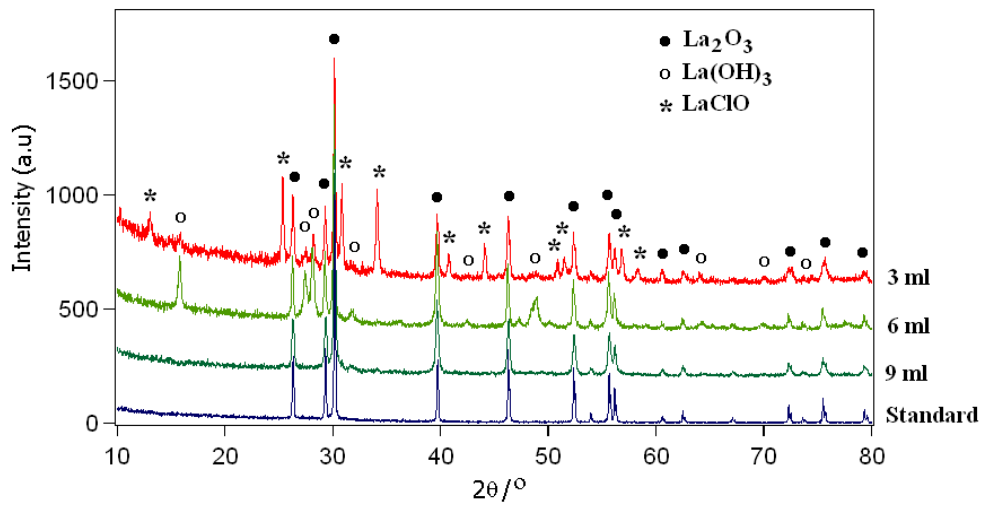
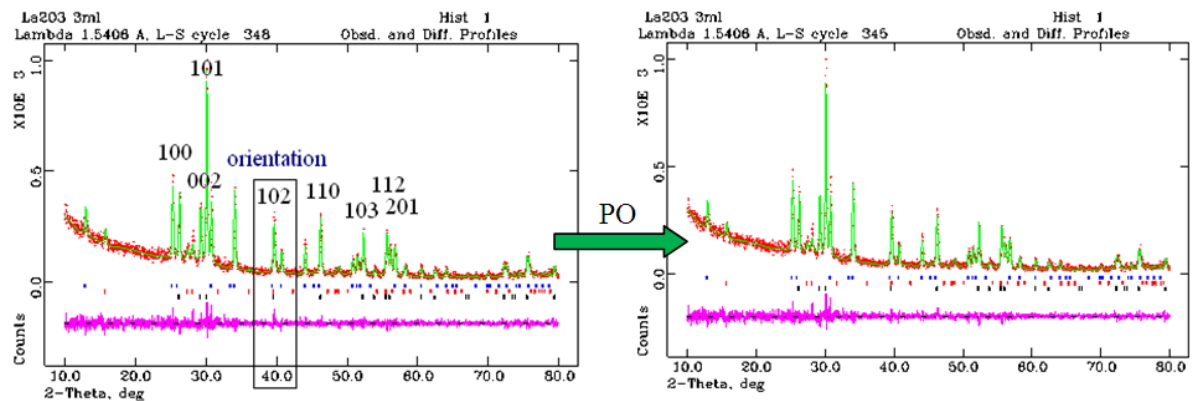
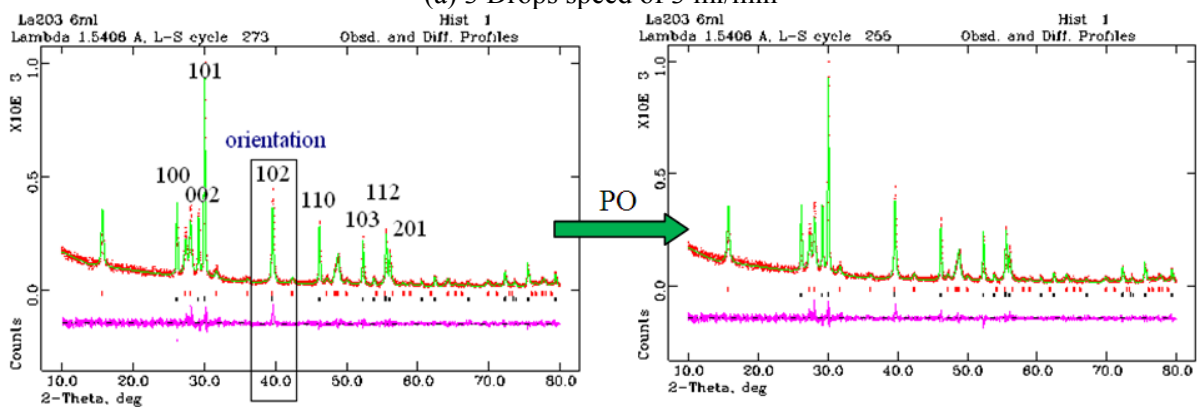


Figure 3. X-ray diffraction pattern of the La₂O₃ nanoneedle with variations in drops speed of (3 ml/min, 6 ml/min, 9 ml/min, and standard)

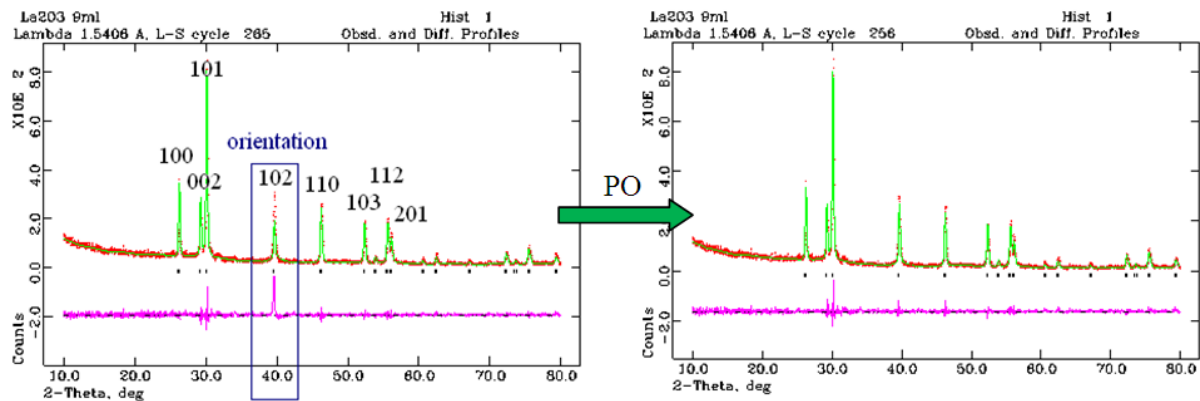
The X-ray diffraction profiles of La₂O₃ nanoneedle are shown in Figure 3 in which respective profiles are 3 ml/min, 6 ml/min, 9 ml/min, and the standard compared. It is shown that the three diffraction patterns exhibit a pattern different between ones each other.



(a) Drops speed of 3 ml/min



(b) Drops speed of 6 ml/min



(c) Drops speed of 9 ml/min

Figure 4. The refinement results of XRD pattern of the La_2O_3 nanoneedles.

Figure 3 shows the results of measurements of X-ray diffraction pattern of the nanoneedle La_2O_3 with variations in drops speed of (3 ml/min, 6 ml/min, 9 ml/min, and standard). Based on the results of the phase identification, the reaction has successfully formed a single phase La_2O_3 on the drops speed of 9 ml/min, while for the drops speed of 3 ml/min and 6 ml/min, the sample can not react perfectly so the sample consists of multi-phases. The results of the phase identification for drops speed of 3 ml/min consist of three phases namely La_2O_3 (lanthanum oxide), $\text{La}(\text{OH})_3$ (lanthanum hydroxide) and LaClO (lanthanum oxychloride), meanwhile for drops speed of 6 ml/min there are two phases namely La_2O_3 and $\text{La}(\text{OH})_3$. Thus, the results require further analysis to determine the changes of the crystal structure parameters, the amount of mass fraction formed, and fitting quality as shown in Figure 4.

Figure 4 shows the results of refinement X-ray diffraction pattern of the nanoneedle La_2O_3 with the variations of drops speed (3 ml/min, 6 ml/min, and 9 ml/min). Qualitative and quantitative analysis refers to the Crystallography Open Database with the card number (COD: 2002286), (COD: 4031381) and (COD: 2101549) respective for phases of La_2O_3 , $\text{La}(\text{OH})_3$ and LaClO .

The complete summary of the results of X-ray diffraction pattern of the nanoneedle La_2O_3 with the variations of drops speed (3 ml/min, 6 ml/min, and 9 ml/min) for all of samples are shown in Table 1.

Table 1. The value of structure parameters, criteria of fit (R_{wp}), goodness of fit (χ^2) and the mass fraction of phase formed in the La_2O_3 nanoneedle with variations of drops speed (3 ml/min, 6 ml/min, and 9 ml/min).

Sample	Phase	Lattice parameter (\AA)			V (\AA^3)	P (g/cm^3)	Fraction wt%	R_{wp} (%)	χ^2
		$a = b$	c	PO					
3 ml/min	La_2O_3	3.9341(2)	6.1275(4)	[102] (0.94)	82.13(1)	5.989	22.97	7.81	1.26
	$\text{La}(\text{OH})_3$	6.5274(3)	3.8494(2)	-	142.0(1)	4.371	15.92		
	LaClO	4.1196(3)	6.8743(8)	-	116.6(2)	5.419	61.11		
6 ml/min	La_2O_3	3.9347(1)	6.1235(3)	[102] (0.82)	82.10(8)	5.691	73.28	7.57	1.25
	$\text{La}(\text{OH})_3$	6.5243(8)	3.8544(6)	-	142.1(1)	4.368	26.72		
9 ml/min	La_2O_3	3.9344(2)	6.1241(4)	[102] (0.76)	82.10(1)	5.371	100.00	7.31	1.15

Figure 4 and Table 1 show that the refinement results of X-ray diffraction pattern has also a good fitting quality. Table 1 shows that based on the refinement of XRD pattern, especially for phases of La_2O_3 , it is concluded for all of the samples, that the lattice parameters, volume of unit cell, and atomic density do not change. It means that the crystal structure of La_2O_3 phase is not deformed due to the effect of drops speed. However, the drops speed affect the total mass fraction of La_2O_3 crystal growth and preferred orientation of La_2O_3 crystal as shown in Figure 5.

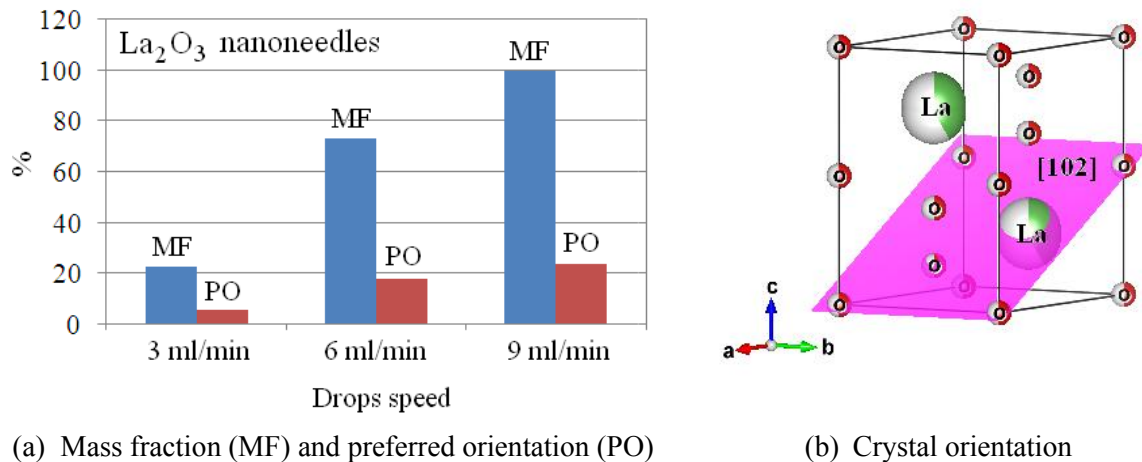


Figure 5. Effect of the drops speed on the mass fraction and preferred orientation of La_2O_3 crystal

In Figure 5, it appears that the La_2O_3 crystal growth and degree of preferred orientation [102] increased in line with the increase of the drops speed. This phenomenon is due to the drops speed of ammonia can affect the amount of La_2O_3 crystal growth. The La_2O_3 crystal has grown naturally on the direction of the field [102]. The present orientation crystal is generally caused by change of particle shape from polygonal to nanoneedles shape.

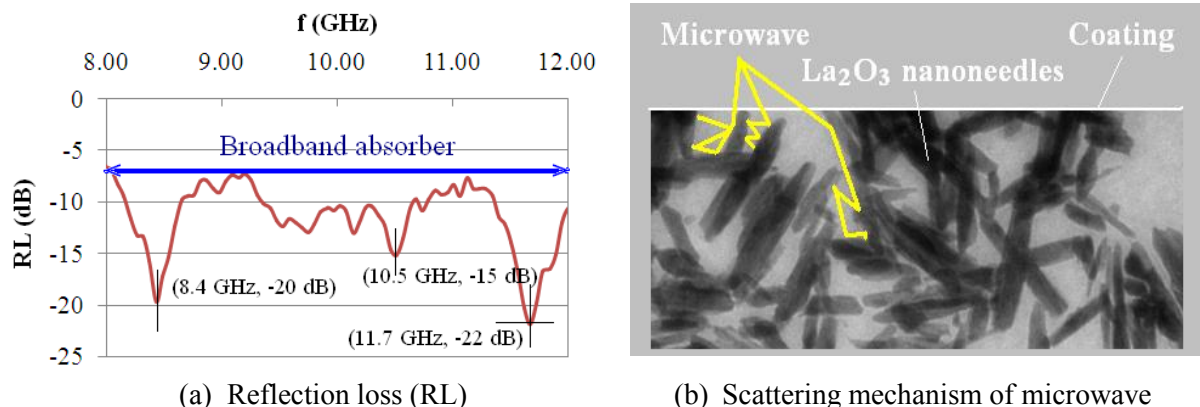


Figure 6. Characteristics of microwave absorber on the La_2O_3 nanoneedles

The intrinsic and extrinsic characteristics of microwave absorber material make a unique phenomenon to be studied. It is because the main requirement is needed as a material absorbing microwave is the presence of intrinsic characteristics (properties of magnetic loss and dielectric loss) on the material in addition to the extrinsic characteristics (factors of the particle geometry). It means that the factor of particle geometry also determines the microwave absorption capability.

Figure 6(a) shows the relation between the reflection loss (RL) of La_2O_3 nanoneedles and the microwave at frequency in range of 8-12 GHz when the thickness of sample is 2 mm. There are at least three absorption peaks observed within the frequency X-band, of which value of the absorption peaks are around -20 dB at 8.4 GHz; -15.0 dB at 10.5 GHz and -22 dB at 11.7 GHz. Meanwhile, the effect of particle geometry on the microwave absorber is shown in Figure 6(b). Figure 6(b) shows that the mechanism of microwave scatters on the particle morphology so that the microwave will not be reflected back to the surface.

4. Conclusion

The synthesis of La_2O_3 nanoparticles has successfully made by using hydrolysis method. Based on the TEM image observations, the morphology of La_2O_3 nanoparticles shaped nanoneedles. The result of morphological of La_2O_3 nanoneedles indicate that better sample is obtained when the sample is synthesized with the drops speed of 9 ml/min. Nanoneedles morphological forms appear more clearly and relatively homogeneous. The average diameter of the particle is about 10 nm with an average length of about 250 nm. The changing shape of the particles from polygonal shape into nanoneedles is affected by the presence of preferred orientation (PO) of crystal on the direction of the field [102]. The factor of the particle geometry also determines the microwave absorber capability. The microwave characteristic of the La_2O_3 nanoneedles has indicated certain microwave absorption properties in the frequency range of 8-12 GHz when the thickness of sample is 2 mm. There are at least three absorption peaks observed within the frequency X-band, of which value of the absorption peaks are around -20 dB at 8.4 GHz; -15.0 dB at 10.5 GHz and -22 dB at 11.7 GHz.

5. References

- [1]. Sumarni, Riesna Prassanti, Kurnia Trinopiawan, Sumiarti and Hafni Lissa N 2011 Eksplorium **32** No. 2 115 – 124
- [2]. Riesna Prassanti 2012 Proceedings of the Seminar on Nuclear Geology and Natural Resources Mines (Indonesia: BATAN) 305-325.
- [3]. Kurnia Setiawan Widana, Bambang Priadi and Yustina Tri Handayani Eksplorium 2014 **35** No. 1 1 - 12
- [4]. Mao G, Zhang H, Li H, Jin J and Niu, S., J. Electrochem. Soc., 2012, **159**, p. J48.
- [5]. Das T, Mahata C, Mallik S, Varma S, Sutradhar G, Bose P K and Maiti C K 2012 J. Electrochem. Soc. **159** p. H323.
- [6]. Rocha K O, Santos J B O, Meira D, Pizani P S, Marques C M P, Zanchet D and Bueno J M C 2012 Appl. Catal. A: General **431** p. 79.
- [7]. Cong-Ju Li, Bin Wanga, Jiao-Na Wang 2012 Journal of Magnetism and Magnetic Materials **324** 1305–1311
- [8]. Shuyuan Zhang, Quanxi Cao 2012 Materials Science and Engineering B **177** 678– 684.
- [9]. Wisnu Ari Adi and Azwar Manaf 2013 Journal of Advanced Materials Research **789** pp 97-100
- [10]. Nurul Taufiqu Rochman and Wisnu Ari Adi 2014 Journal of Advanced Materials Research Vol. **896** pp 423-427
- [11]. Zheng D, Shi J, Lu X and Wang C 2010 Cryst. Engin. Commun. **10** p. 4066
- [12]. Wu Y, Chen Y and Zhou J 2013 Mater. Lett. **95** p. 5.
- [13]. Khosrow pour F, Aghazadeh M, Dalvand S and Sabour B 2013 Mater. Lett **104** pp. 61–63.
- [14]. Aghazadeh M, Malek Barmi A A, Mohammad Shiri H and Sedaghat S 2013 Ceram. Int. **39** p. 1045.
- [15]. Jamali Sheini F and Yousefi R 2013 Ceram. Int. **39** p. 3715.
- [16]. Cong-Ju Li, Bin Wanga, Jiao-Na Wang, 2012 Journal of Magnetism and Magnetic Materials **324** 1305–1311
- [17]. Toby B H 2001 EXPGUI A Graphical User Interface for GSAS J. Appl. Crystallogr. **34** 210-221
- [18]. Mazloumi M, Zanganeh S, Kajbafvala A, Shayegh M R and Sadrnezhaad S K 2008 IJE Transactions B: Applications **21** No. 2 169-176.

Acknowledgements

The authors gratefully acknowledge the support of the Centre for Science and Technology of Advanced Materials, BATAN for the research facilities.